JGR Solid Earth

RESEARCH ARTICLE
10.1029/2018JB016778

Effects of Induced Stress on Seismic Waves: Validation Based on Ab Initio Calculations

Jeroen Tromp[1], Michel L. Marcondes[2], Renata M. M. Wentzcovitch[2,3], and Jeannot Trampert[4]

[1]Department of Geosciences and Program in Applied & Computational Mathematics, Princeton University, Princeton, NJ, USA, [2]Department of Earth and Environmental Sciences, Lamont-Doherty Earth Observatory, Columbia University in the City of New York, Palisades, NY, USA, [3]Applied Physics and Applied Mathematics Department, Columbia University, New York, NY, USA, [4]Department of Earth Sciences, Utrecht University, Utrecht, The Netherlands

Abstract When a continuum is subjected to an induced stress, the equations that govern seismic wave propagation are modified in two ways. First, the equation of conservation of linear momentum gains terms related to the induced deviatoric stress, and, second, the elastic constitutive relationship acquires terms linear in the induced stress. This continuum mechanics theory makes testable predictions with regard to stress-induced changes in the elastic tensor. Specifically, it predicts that induced compression linearly affects the prestressed moduli with a slope determined by their local adiabatic pressure derivatives and that induced deviatoric stress produces anisotropic compressional and shear wave speeds. In this article we successfully compare such predictions against ab initio mineral physics calculations for NaCl and MgO.

Key Points:
- We compare ab initio calculations of effects of induced stress on elastic parameters with predictions based on a continuum mechanics theory
- We find that the two methods are in good agreement, without the need of higher-order theories of elasticity
- The theory currently in use for accommodating the effects on nonhydrostatic prestress on seismic wave propagation needs to be modified

Correspondence to:
J. Tromp,
jtromp@princeton.edu

Citation:
Tromp, J., Marcondes, M. L., Wentzcovitch, R. M. M., & Trampert, J. (2019). Effects of induced stress on seismic waves: Validation based on ab initio calculations. *Journal of Geophysical Research: Solid Earth*, *124*, 729–741. https://doi.org/10.1029/2018JB016778

Received 25 SEP 2018
Accepted 8 JAN 2019
Accepted article online 10 JAN 2019
Published online 23 JAN 2019

1. Introduction

The effects of changes in stress on seismic wave propagation are commonly described in two different contexts. One focuses on stress effects on preexisting or induced cracks, which manifest themselves in the form of seismic anisotropy (e.g., Bruner, 1976; Henyey & Pomphrey, 1982; Nur, 1971; O'Connell & Budiansky, 1974; Zheng, 2000). In the other context of mineral physics, the effects of stress changes are frequently captured based on third-order elasticity theory (Bogardus, 1965; Egle & Bray, 1976; Hughes & Kelly, 1953; Murnaghan, 1951; Wang & Li, 2009), requiring knowledge of higher-order elastic constants, which are not easily measured in the laboratory (e.g., Renaud et al., 2012; Telichko et al., 2017). We propose an alternative approach in the latter context without introducing higher-order derivatives.

In a previous article, Tromp and Trampert (2018) considered the effects of induced stress on seismic wave propagation based on a continuum mechanics theory motivated by the accommodation of prestress in global seismology. Prestress refers to Earth's state of stress prior to an earthquake, whereas induced stress refers to an additional stress superimposed on a background state of stress. The hydrostatic prestress (pressure) can be large (tens of gigapascals in Earth's mantle), but the nonhydrostatic or deviatoric prestress is believed to be comparably small ($<$ 0.5 GPa, i.e., a fraction of a percent of the shear modulus; Dahlen & Tromp, 1998, section 3.11.1).

As first discussed in Dahlen, (1972a, 1972b) and also in Dahlen & Tromp, 1998 (1998, sections 3.3.2 and 3.6.2), prestress affects both the equation of conservation of linear momentum and the constitutive relationship.

Building on the approach in global seismology, Tromp and Trampert (2018) developed a theory describing the effects of an induced stress on seismic wave propagation. They explored such effects both from a forward modeling point of view and from the perspective of the inverse problem, and they show examples of observable effects of prestress on seismic wave propagation in the setting of a hydrocarbon field, where the deviatoric prestress is estimated to reach 2% of the shear modulus. Additionally, they demonstrate that the original theory developed by Dahlen needs to be modified to accommodate pressure derivatives of the moduli, which affect the magnitude of the induced anisotropic wave speeds. The modified theory of Tromp and Trampert (2018) makes testable predictions, and in this article we benchmark such predictions against ab initio mineral physics calculations. Basic effects of changes in pressure on seismic wave speeds have been known for a long time (e.g., Birch, 1961; Nur & Simmons, 1969), and such effects have been observed in

laboratory (e.g., Eberhart-Phillips et al., 1989; Verdon et al., 2008) and field studies (e.g., Fazio et al., 1973; Silver et al., 2007). Here, we also consider the effects of nonhydrostatic stress changes.

We assume a medium to be prestressed; that is, all elastic constants are at pressure P. We then subject the medium to an additional induced stress $\mathbf{T}^0$. Our theory, summarized below, relates the elastic constants in the prestressed state to the elastic constants in the prestressed plus induced stress state. All we need to know are the adiabatic pressure derivatives of the elastic constants in the prestressed state. The underlying assumption is that the induced stress is a linear perturbation on top of the prestress, and, consequently, that linear conservation laws hold. This means that our approach is strictly local, as opposed to more global descriptions based on higher-order elasticity (e.g., Johnson & Rasolofosaon, 1996; Prioul et al., 2004).

2. Effects of Induced Stress on Seismic Waves

Induced stress affects seismic wave propagation in two ways. First, it modifies the equation of motion, and, second, it modifies the constitutive relationship. In this section, we summarize the effects of stress changes on seismic wave propagation; for a more in-depth discussion, see Tromp and Trampert (2018).

We express the symmetric induced stress, $\mathbf{T}^0$, in the form

$$\mathbf{T}^0 = -p^0\,\mathbf{I} + \boldsymbol{\tau}^0, \tag{1}$$

where $\mathbf{I}$ denotes the identity tensor, p^0 the induced pressure,

$$p^0 = -\frac{1}{3}\,\mathrm{tr}(\mathbf{T}^0), \tag{2}$$

and τ^0 the symmetric trace-free induced deviatoric stress,

$$\boldsymbol{\tau}^0 = \mathbf{T}^0 - \frac{1}{3}\,\mathrm{tr}(\mathbf{T}^0)\,\mathbf{I}. \tag{3}$$

Before inducing stress, the equation of motion is given by

$$\rho\,\partial_t^2\mathbf{s} - \boldsymbol{\nabla}\cdot\mathbf{T} = \mathbf{0}, \tag{4}$$

where ρ denotes the mass density and $\mathbf{s}$ the displacement. The stress tensor, $\mathbf{T}$, is linearly related to the infinitesimal strain tensor,

$$\boldsymbol{\epsilon} = \frac{1}{2}[\boldsymbol{\nabla}\,\mathbf{s} + (\boldsymbol{\nabla}\,\mathbf{s})^T)], \tag{5}$$

(a superscript T denotes the transpose) via Hooke's law:

$$\mathbf{T} = \boldsymbol{\Gamma} : \boldsymbol{\epsilon}. \tag{6}$$

The fourth-order elastic tensor, Γ , exhibits the symmetries

$$\Gamma_{ijk\ell} = \Gamma_{jik\ell} = \Gamma_{ij\ell k} = \Gamma_{k\ell ij}, \tag{7}$$

which, in the most general case, reduce the number of independent parameters from 81 to 21. It is often convenient to express the elastic tensor in terms of its isotropic and purely anisotropic parts as

$$\Gamma_{ijk\ell} = (\kappa - \frac{2}{3}\,\mu)\,\delta_{ij}\,\delta_{k\ell} + \mu\,(\delta_{ik}\,\delta_{j\ell} + \delta_{i\ell}\,\delta_{jk}) + \gamma_{ijk\ell}, \tag{8}$$

where κ and μ denote the isotropic bulk and shear moduli, respectively, and $\gamma_{ijk\ell}$ a purely anisotropic contribution. The elements $\gamma_{ijk\ell}$ exhibit the same symmetries as the elements $\gamma_{ijk\ell}$, and for purely isotropic media $\gamma_{ijk\ell} = 0$.

As discussed in Tromp and Trampert (2018), the equation of motion in a medium with an additional induced stress takes the modified form (see also Dahlen & Tromp, 1998, equation 3.58 without density and gravity perturbations or rotational terms)

$$\rho\,\partial_t^2\mathbf{s} - \boldsymbol{\nabla}\cdot\mathbf{T}^{\mathrm{L1}} - \boldsymbol{\nabla}[\mathbf{s}\cdot(\boldsymbol{\nabla}\cdot\boldsymbol{\tau}^0)] + \boldsymbol{\nabla}\cdot(\mathbf{s}\cdot\boldsymbol{\nabla}\,\boldsymbol{\tau}^0) = \mathbf{0}, \tag{9}$$

and Hooke's law is modified to become

$$\mathbf{T}^{\mathrm{L1}} = \mathbf{\Gamma} : \boldsymbol{\epsilon} + \Delta\mathbf{T}. \tag{10}$$

The quantity $\mathbf{T}^{\mathrm{L1}}$ denotes the symmetric incremental Lagrangian Cauchy stress (Dahlen & Tromp, 1998), and the effects of the induced stress are captured by the symmetric second-order tensor

$$\begin{aligned}\Delta\mathbf{T} = \; & [(\kappa' - \frac{2}{3}\mu')\mathrm{tr}(\boldsymbol{\epsilon})\mathbf{I} + 2\mu'\boldsymbol{\epsilon}]p^0 + \frac{1}{2}[(\boldsymbol{\tau}^0 : \boldsymbol{\epsilon})\mathbf{I} - \mathrm{tr}(\boldsymbol{\epsilon})\boldsymbol{\tau}^0] \\ & - \frac{1}{2}(\kappa' - \frac{2}{3}\mu')[(\boldsymbol{\tau}^0 : \boldsymbol{\epsilon})\mathbf{I} + \mathrm{tr}(\boldsymbol{\epsilon})\boldsymbol{\tau}^0] - \mu'(\boldsymbol{\tau}^0 \cdot \boldsymbol{\epsilon} + \boldsymbol{\epsilon} \cdot \boldsymbol{\tau}^0) \\ & + \boldsymbol{\omega} \cdot \boldsymbol{\tau}^0 - \boldsymbol{\tau}^0 \cdot \boldsymbol{\omega}.\end{aligned} \tag{11}$$

Note that the two additional terms in the equation of motion (9) depend only on the induced deviatoric stress, τ^0. The modification of Hooke's law, captured by equation (11), involves adiabatic pressure derivatives of the isotropic moduli, κ' and μ', the induced pressure and deviatoric stress, p^0 and τ^0, and the infinitesimal strain tensor (5) and the antisymmetric infinitesimal vorticity tensor

$$\boldsymbol{\omega} = -\frac{1}{2}[\boldsymbol{\nabla}\mathbf{s} - (\boldsymbol{\nabla}\mathbf{s})^T)]. \tag{12}$$

The goal of this paper is to compare predictions based on the theory summarized in this section with ab initio mineral physics calculations.

3. Elastic Tensor Under Induced Stress

Ab initio calculations are based on the assumption that the Lagrangian internal energy per unit mass, U^L, is quadratic in the Lagrangian strain tensor,

$$\mathbf{E}^{\mathrm{L}} = \frac{1}{2}[\boldsymbol{\nabla}\mathbf{s} + (\boldsymbol{\nabla}\mathbf{s})^T)] + \frac{1}{2}(\boldsymbol{\nabla}\mathbf{s}) \cdot (\boldsymbol{\nabla}\mathbf{s})^T, \tag{13}$$

that is (e.g., Barron & Klein, 1965; Dahlen & Tromp, 1998; Karki et al., 2001),

$$\rho^0 U^{\mathrm{L}} = \mathbf{T}^0 : \mathbf{E}^{\mathrm{L}} + \frac{1}{2}\mathbf{E}^{\mathrm{L}} : \mathbf{\Xi} : \mathbf{E}^{\mathrm{L}}. \tag{14}$$

Here ρ^0 denotes the density before straining the material, and $\mathbf{T}^0$ denotes the induced stress. For convenience, we have assumed that the Lagrangian internal energy density vanishes in the absence of strain.

The symmetric second Piola-Kirchhoff stress is defined in terms of the Lagrangian internal energy via

$$\mathbf{T}^{\mathrm{SK}} = \rho^0 \frac{\partial U^{\mathrm{L}}}{\partial \mathbf{E}^{\mathrm{L}}} = \mathbf{T}^0 + \mathbf{T}^{\mathrm{SK1}}, \tag{15}$$

where $\mathbf{T}^{\mathrm{SK1}}$ denotes the symmetric incremental second Piola-Kirchhoff stress, namely,

$$\mathbf{T}^{\mathrm{SK1}} = \mathbf{\Xi} : \mathbf{E}^{\mathrm{L}}. \tag{16}$$

The components of the fourth-order tensor $\mathbf{\Xi}$ are given by

$$\Xi_{ijk\ell} = \rho^0 \frac{\partial^2 U^{\mathrm{L}}}{\partial E^{\mathrm{L}}_{ij}\, \partial E^{\mathrm{L}}_{k\ell}}. \tag{17}$$

Equation (17) implies that $\mathbf{\Xi}$ exhibits the usual symmetries, namely,

$$\Xi_{ijk\ell} = \Xi_{jik\ell} = \Xi_{ij\ell k} = \Xi_{k\ell ij}. \tag{18}$$

The incremental Lagrangian Cauchy stress (10) and the incremental second Piola-Kirchhoff stress (16) are related via (Dahlen & Tromp, 1998, equation 3.37)

$$\mathbf{T}^{\mathrm{SK1}} = \mathbf{T}^{\mathrm{L1}} + \mathbf{T}^0\,\boldsymbol{\nabla}\cdot\mathbf{s} - (\boldsymbol{\nabla}\,\mathbf{s})^T\cdot\mathbf{T}^0 - \mathbf{T}^0\cdot\boldsymbol{\nabla}\,\mathbf{s}. \tag{19}$$

The last equation ties the ab initio calculations to the equation of motion (9).

Tromp and Trampert (2018) demonstrate that the tensor $\Xi_{ijk\ell}$ may be expressed in terms of the unstressed elastic tensor $\Gamma_{ijk\ell}$, the induced stress $\mathbf{T}^0$, and the pressure derivatives κ' and μ' as

$$\begin{aligned}\Xi_{ijk\ell} = \;& \Gamma_{ijk\ell} + \frac{1}{2}(1-\kappa'+\frac{2}{3}\mu')(T^0_{ij}\,\delta_{k\ell} + T^0_{k\ell}\,\delta_{ij}) \\ & - \frac{1}{2}(1+\mu')(T^0_{ik}\,\delta_{j\ell} + T^0_{jk}\,\delta_{i\ell} + T^0_{i\ell}\,\delta_{jk} + T^0_{j\ell}\,\delta_{ik}).\end{aligned} \tag{20}$$

This theory makes testable predictions: given an induced stress $\mathbf{T}^0$ and pressure derivatives κ' and μ', equation (20) implies changes in the elastic tensor that may be benchmarked against ab initio mineral physics calculations.

Before doing so, we wish to generalize equation (20). The effects of the induced stress are captured by the terms

$$\begin{aligned}&\frac{1}{2}(T^0_{ij}\,\delta_{k\ell} + T^0_{k\ell}\,\delta_{ij}) - \frac{1}{2}(T^0_{ik}\,\delta_{j\ell} + T^0_{jk}\,\delta_{i\ell} + T^0_{i\ell}\,\delta_{jk} + T^0_{j\ell}\,\delta_{ik}) \\ &- \frac{1}{2}(\kappa' - \frac{2}{3}\mu')(T^0_{ij}\,\delta_{k\ell} + T^0_{k\ell}\,\delta_{ij}) - \frac{1}{2}\mu'(T^0_{ik}\,\delta_{j\ell} + T^0_{jk}\,\delta_{i\ell} + T^0_{i\ell}\,\delta_{jk} + T^0_{j\ell}\,\delta_{ik}),\end{aligned}$$

which may be rewritten in the form

$$\frac{1}{2}(T^0_{ij}\,\delta_{k\ell} + T^0_{k\ell}\,\delta_{ij}) - \frac{1}{2}(T^0_{ik}\,\delta_{j\ell} + T^0_{jk}\,\delta_{i\ell} + T^0_{i\ell}\,\delta_{jk} + T^0_{j\ell}\,\delta_{ik}) - \frac{1}{4}\Theta_{ijk\ell mn}\,T^0_{mn},$$

where

$$\begin{aligned}\Theta_{ijk\ell mn} = \;& \delta_{jn}[(\kappa' - \frac{2}{3}\mu')\delta_{im}\,\delta_{k\ell} + \mu'(\delta_{km}\delta_{i\ell} + \delta_{\ell m}\,\delta_{ik})] \\ & + \delta_{in}[(\kappa' - \frac{2}{3}\mu')\delta_{jm}\,\delta_{k\ell} + \mu'(\delta_{km}\,\delta_{j\ell} + \delta_{\ell m}\,\delta_{jk})] \\ & + \delta_{\ell n}[(\kappa' - \frac{2}{3}\mu')\delta_{km}\,\delta_{ij} + \mu'(\delta_{im}\,\delta_{jk} + \delta_{jm}\,\delta_{ik})] \\ & + \delta_{kn}[(\kappa' - \frac{2}{3}\mu')\delta_{\ell m}\,\delta_{ij} + \mu'(\delta_{im}\,\delta_{j\ell} + \delta_{jm}\,\delta_{i\ell})].\end{aligned} \tag{21}$$

The tensor $\Theta_{ijk\ell mn}$ must exhibit the "elastic" symmetries

$$\Theta_{ijk\ell mn} = \Theta_{jik\ell mn} = \Theta_{ij\ell kmn} = \Theta_{k\ell ijmn}, \tag{22}$$

as well as the symmetries imposed by the induced stress,

$$\Theta_{ijk\ell mn} = \Theta_{ijk\ell nm}. \tag{23}$$

We recognize terms of the form $(\kappa' - \frac{2}{3}\mu')\delta_{im}\,\delta_{k\ell} + \mu'(\delta_{km}\delta_{i\ell} + \delta_{\ell m}\,\delta_{ik})$ as pressure derivatives of an isotropic elastic tensor. This motivates a generalization of the tensor $\Theta_{ijk\ell mn}$ while retaining its required symmetries (22) and (23), namely,

$$\begin{aligned}\Theta_{ijk\ell mn} = \;& \frac{1}{2}(\delta_{jn}\Gamma'_{imk\ell} + \delta_{jm}\Gamma'_{ink\ell} + \delta_{in}\Gamma'_{jmk\ell} + \delta_{im}\Gamma'_{jnk\ell} \\ & + \delta_{\ell n}\Gamma'_{kmij} + \delta_{\ell m}\Gamma'_{knij} + \delta_{kn}\Gamma'_{\ell mij} + \delta_{km}\Gamma'_{\ell nij}),\end{aligned} \tag{24}$$

where $\Gamma'_{ijk\ell}$ denote pressure derivatives of the elements of the elastic tensor. Thus, the generalization of equation (20) is

$$\begin{aligned}\Xi_{ijk\ell} = \;& \Gamma_{ijk\ell} + \Gamma'_{ijk\ell}\,p^0 - p^0(\delta_{ij}\,\delta_{k\ell} - \delta_{ik}\,\delta_{j\ell} - \delta_{jk}\,\delta_{i\ell}) \\ & + \frac{1}{2}(\tau^0_{ij}\,\delta_{k\ell} + \tau^0_{k\ell}\,\delta_{ij}) - \frac{1}{2}(\tau^0_{ik}\,\delta_{j\ell} + \tau^0_{jk}\,\delta_{i\ell} + \tau^0_{i\ell}\,\delta_{jk} + \tau^0_{j\ell}\,\delta_{ik}) \\ & - \frac{1}{4}(\Gamma'_{imk\ell}\,\tau^0_{mj} + \Gamma'_{jmk\ell}\,\tau^0_{mi} + \Gamma'_{kmij}\,\tau^0_{m\ell} + \Gamma'_{\ell mij}\,\tau^0_{mk}).\end{aligned} \tag{25}$$

The ab initio calculations will be based on the tensor elements $\Xi_{ijk\ell}$ and its pressure derivatives $\Xi'_{ijk\ell}$. Upon differentiating equation (25) with respect to pressure, we see that the pressure derivative $\Xi'_{ijk\ell}$ is related to the pressure derivative $\Gamma'_{ijk\ell}$ via

$$\Xi'_{ijk\ell} = \Gamma'_{ijk\ell} - (\delta_{ij}\,\delta_{k\ell} - \delta_{ik}\,\delta_{j\ell} - \delta_{jk}\,\delta_{i\ell}). \tag{26}$$

Thus, in terms $\Xi'_{ijk\ell}$ rather than $\Gamma'_{ijk\ell}$, we find that changes in the elastic tensor induced by the stress, $\delta\Xi_{ijk\ell} = \Xi_{ijk\ell} - \Gamma_{ijk\ell}$, are given by

$$\delta\Xi_{ijk\ell} = \Xi'_{ijk\ell}\,p^0 - \frac{1}{4}(\Xi'_{imk\ell}\,\tau^0_{mj} + \Xi'_{jmk\ell}\,\tau^0_{mi} + \Xi'_{kmij}\,\tau^0_{m\ell} + \Xi'_{\ell mij}\,\tau^0_{mk}). \tag{27}$$

This is the equation that we compare against ab initio calculations in the next section. We shall consider prestressed samples of NaCl and MgO under mantle conditions and subject them to an additional induced stress.

4. Ab Initio Calculations

Ab initio methods based on Density Functional Theory (Hohenberg & Kohn, 1964; Kohn & Sham, 1965) have been used to calculate elastic coefficients of complex materials since the mid-1990s (Wentzcovitch & Price, 1996). Such calculations are currently routinely performed at high pressures and temperatures (Wentzcovitch et al., 2010). Here we apply these methods to compute the static elastic tensor under hydrostatic and nonhydrostatic conditions. The present calculations do not include vibrational contributions to the elastic coefficients. They are strictly static lattice calculations (zero kelvin without zero-point motion effects). Here we present ab initio calculations of the elastic tensor components for NaCl and MgO in the rock-salt cubic structure. NaCl is commonly encountered in offshore exploration seismology in the form of salt domes, and MgO is one of the primary constituents of the Earth's lower mantle. We used the Quantum ESPRESSO software to perform the calculations and the local-density approximation functional for the exchange-correlation energy (Giannozzi et al., 2009). The electronic wave functions of Mg and O were calculated using norm-conserving pseudopotentials. For NaCl we used the projector augmented wave method. We sampled the NaCl electronic states on displaced 8 ×8× 8 **k**-mesh, using an energy cutoff of 100 Ry. For MgO, we used a 12 ×12× 12 displaced **k**-mesh with energy cutoff of 160 Ry. These plane wave energy cutoffs and **k**-meshes are very high in general, but the small differences in the stress tensor caused by the prestressed case requires extra accuracy. Both crystals have cubic symmetry; therefore, there are only three independent elastic coefficients, namely, Ξ_{1111}, Ξ_{1122}, and Ξ_{2323}. In Voigt notation, the elastic matrix takes the symmetric form

$$\begin{bmatrix} \Xi_{1111} & \Xi_{1122} & \Xi_{1122} & 0 & 0 & 0 \\ & \Xi_{1111} & \Xi_{1122} & 0 & 0 & 0 \\ & & \Xi_{1111} & 0 & 0 & 0 \\ & & & \Xi_{2323} & 0 & 0 \\ & & & & \Xi_{2323} & 0 \\ & & & & & \Xi_{2323} \end{bmatrix}. \tag{28}$$

The three elastic moduli of NaCl and MgO under hydrostatic conditions in relevant pressure ranges are shown in Figure 1, while the associated pressure derivatives are shown in Figure 2. These results are obtained by calculating the elastic parameters at 12 equally spaced pressures identified by the dots in Figure 1. The crystal cells are optimized at each pressure with variable cell shape molecular dynamics (Wentzcovitch, 1991; Wentzcovitch et al., 1993), and pressure is calculated by fitting the Lagrangian energy per unit volume, $E = \rho^0\,U^L$, as a function of volume, V, to a third-order finite strain equation of state (Poirer, 2000):

$$E(V) = E^0 + \frac{9}{2}V^0\kappa^0 f^2\left[1 + f\left(\kappa'^0 - 4\right)\right], \tag{29}$$

where

$$f = \frac{1}{2}[(V^0/V)^{\frac{2}{3}} - 1], \tag{30}$$

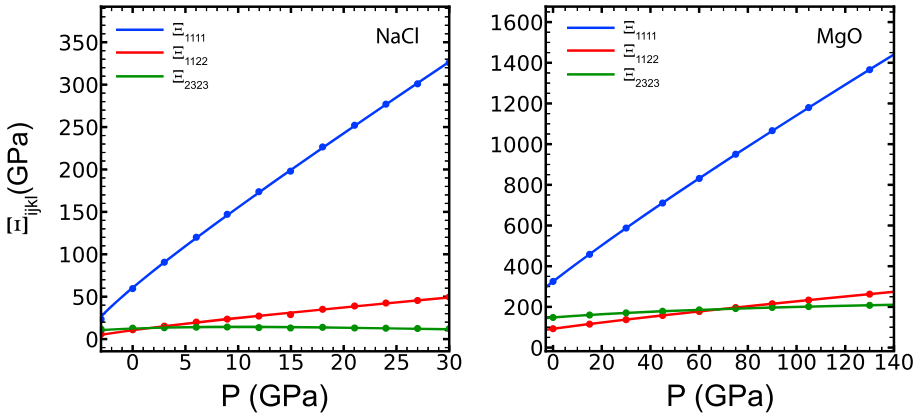

Figure 1. Elastic moduli of NaCl (left) and MgO (right), which have cubic symmetry, plotted as a function of pressure in the range from −3 to 30 GPa. The colored dots correspond to the 10 pressures that were used for interpolation based upon the finite strain equation of state (29).

thereby determining E^0, V^0, κ^0 and κ'^0. Upon differentiating equation (29) with respect to V, analytical expressions for pressure P and bulk modulus κ as a function of volume are obtained, using the thermodynamic identities

$$P(V) = -\left(\frac{\partial E}{\partial V}\right)_S = 3\kappa^0 f(1+2f)^{\frac{5}{2}}\left[1+\frac{3}{2}\left(\kappa'^0-4\right)\right], \tag{31}$$

and (discarding second-order terms in f)

$$\kappa(V) = -V\left(\frac{\partial P}{\partial V}\right)_T = \kappa^0(1+2f)^{\frac{5}{2}}\left[1+\left(3\kappa'^0-5\right)f\right]. \tag{32}$$

Here S and T denote entropy and temperature, respectively, where in this case $T = 0$ K and S is constant and equal to 0. At each pressure, the elastic matrix (28) was calculated by applying positive and negative Lagrangian strains (E^{L}_{kl}) of 0.5% and calculating the stress tensor with the stress theorem (Nielsen & Martin, 1985). The elastic coefficients may be obtained via the linear stress-strain relationship (16) (Karki et al., 2001; Wentzcovitch & Price, 1996); that is,

$$T^{\mathrm{SK1}}_{ij} = T^{\mathrm{SK}}_{ij} + P\delta_{ij} = \Xi_{ijkl}E^{\mathrm{L}}_{kl}, \tag{33}$$

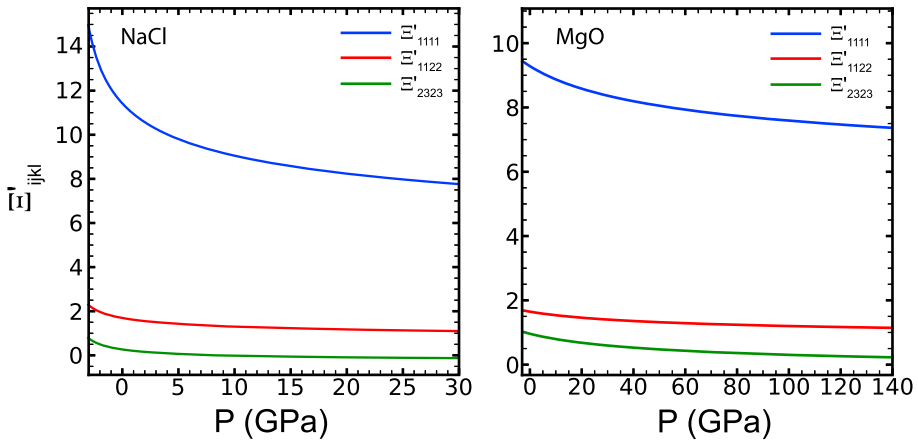

Figure 2. Pressure derivatives of the three elastic moduli of NaCl (left) and MgO (right) plotted as a function of pressure in the range from −3 to 30 GPa.

where P denotes the pressure associated with the isotropic prestress $-P\mathbf{I}$.

The elastic parameters are assumed to have the same volume dependence as the bulk modulus; therefore,

$$\Xi_{ijkl}(V) = \Xi^0_{ijkl}(1+2f)^{\frac{5}{2}}\left[1+\left(3\Xi'^0_{ijkl}-5\right)f\right]. \tag{34}$$

The calculated values of $\Xi_{ijk\ell}$ are fitted to equation (34), which determines $\Xi^0_{ijk\ell}$ and $\Xi'^0_{ijk\ell}$. Pressure derivatives of the elastic moduli, $\Xi'_{ijk\ell}$, are calculated analytically via

$$\Xi'_{ijk\ell} = \frac{1}{3\kappa}\Xi^0_{ijk\ell}(1+2f)^{\frac{5}{2}}\left[5+\left(3\Xi'^0_{ijk\ell}-5\right)(1+7f)\right]. \tag{35}$$

At this point, we have the pressure derivatives we need to use equation (27) to predict changes in the elastic parameters due to induced stresses. Now that the pressure dependence of the elastic moduli has been established, we can subject our sample to an induced stress at a chosen pressure. In other words, we take a sample at pressure P, having cubic elastic moduli $\Xi_{ijk\ell}(P)$ of the form (28), and subject it to an induced stress $\mathbf{T}^0$ of the form (1). Explicitly, we have

$$T^{\mathrm{SK1}}_{ij} = T^{\mathrm{SK}}_{ij} + P\delta_{ij} + p^0\delta_{ij} - \tau^0_{ij} = (\Xi_{ijkl} + \delta\Xi_{ijk\ell})E^{\mathrm{L}}_{kl}. \tag{36}$$

The presstressed sample at pressure P is deformed by the induced stress, $-p^0\delta_{ij} + \tau^0_{ij}$, and the resulting changes in the elastic moduli, $\delta\Xi_{ijk\ell}$, are recorded.

4.1. Induced Pressure

The first test is aimed at confirming the predicted induced pressure dependence of the elastic parameters. Equation (27) predicts that this change is of the simple form

$$\delta\Xi_{ijk\ell} = \Xi'_{ijk\ell}p^0. \tag{37}$$

With this goal in mind, the NaCl and MgO samples are subjected to a strain of the form

$$\epsilon_{11} = \epsilon_{22} = \epsilon_{33} = \epsilon^0 = 0.01. \tag{38}$$

The resulting induced pressure is of the form

$$p^0 = -(\Xi_{1111} + 2\Xi_{1122})\epsilon^0, \tag{39}$$

and there is no induced deviatoric stress: $\tau^0 = \mathbf{0}$. According to equation (37), the expected changes in the three elastic moduli are given by

$$\delta\Xi_{1111} = \Xi'_{1111}p^0, \tag{40}$$

$$\delta\Xi_{1122} = \Xi'_{1122}p^0, \tag{41}$$

$$\delta\Xi_{2323} = \Xi'_{2323}p^0. \tag{42}$$

In Figure 3 we compare these predictions against ab initio calculations, and we conclude that the two methods are in excellent agreement for both NaCl and MgO. Error bars were assigned to the ab initio calculations and the continuum mechanics predictions based on an analysis summarized in Appendix A.

4.2. Induced Uniaxial Stretch

In the next test we subject the NaCl and MgO samples to a uniaxial stretch in the z direction, resulting in a strain given by

$$\epsilon_{33} = \epsilon^0 = 0.01. \tag{43}$$

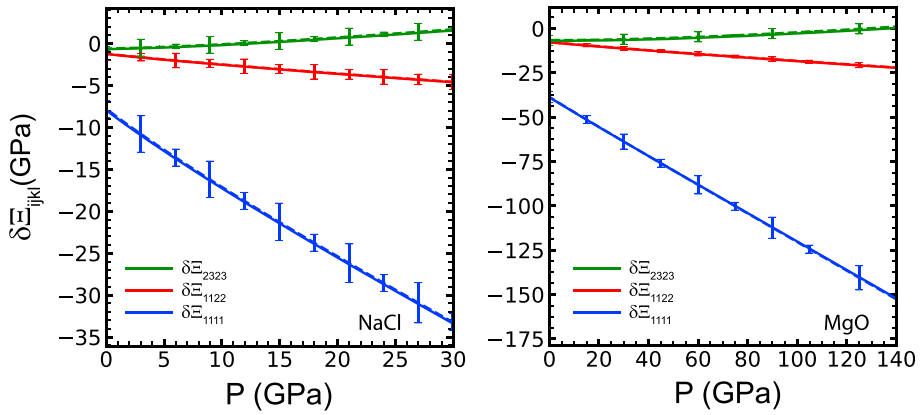

Figure 3. Comparison of changes in the elastic moduli of NaCl (left) and MgO (right) due to an induced pressure determined based upon ab initio calculations (solid lines) and continuum mechanics (dashed lines) as a function of pressure in the range from −3 to 30 GPa. At a given pressure, a cubic NaCl or MgO sample is subjected to a strain of the form $\epsilon_{11} = \epsilon_{22} = \epsilon_{33} = 0.01$, which results in an additional induced pressure. The resulting changes in the moduli are determined based on ab initio calculations as well as equation (37). Error bars for the ab initio calculations and the continuum mechanics predictions are determined based on an analysis discussed in Appendix A. The two sets of error bars are staggered for clarity of viewing.

In this case the induced stress (1) involves both an induced pressure and an induced deviatoric stress, namely,

$$p^0 = -\frac{1}{3}(\Xi_{1111} + 2\Xi_{1122})\epsilon^0, \tag{44}$$

$$\tau^0_{11} = \tau^0_{22} = \tau^0 = -\frac{1}{3}(\Xi_{1111} - \Xi_{1122})\epsilon^0, \tag{45}$$

$$\tau^0_{33} = -2\tau^0. \tag{46}$$

According to equation (39), the expected changes in the elastic moduli are given by

$$\delta\Xi_{1111} = \delta\Xi_{2222} = \Xi'_{1111}(p^0 - \tau^0), \tag{47}$$

$$\delta\Xi_{1122} = \Xi'_{1122}(p^0 - \tau^0), \tag{48}$$

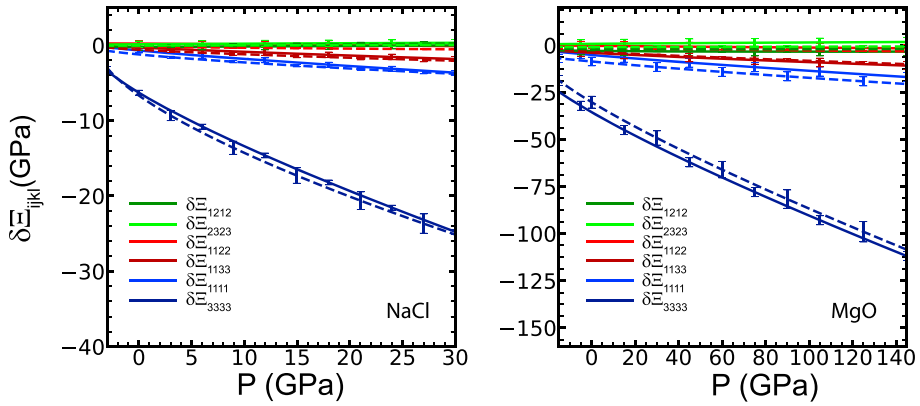

Figure 4. Comparison of changes in the elastic moduli of NaCl (left) and MgO (right) due to a uniaxial stretch determined based upon ab initio calculations (solid lines) and continuum mechanics (dashed lines) as a function of pressure in the range from −3 to 30 GPa. At a given pressure, a cubic NaCl or MgO sample is subjected to a uniaxial strain of the form $\epsilon_{33} = 0.01$, which results in an additional induced stress. The resulting changes in the moduli are determined based on ab initio calculations as well as equation (27).

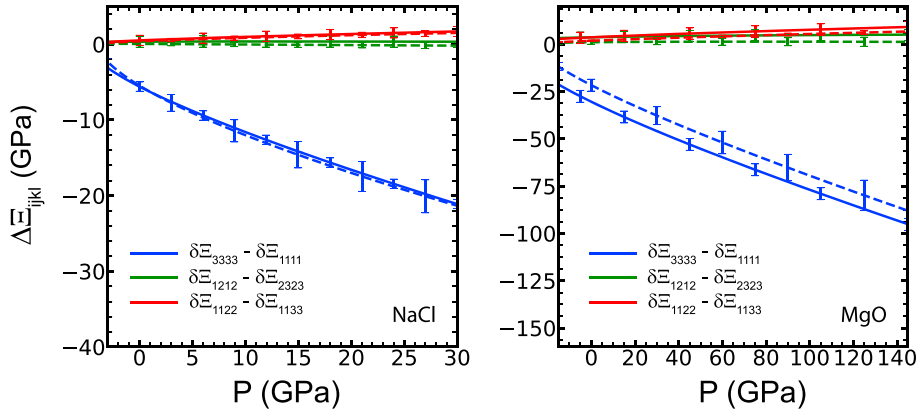

Figure 5. Comparison of differences between changes in the elastic moduli of NaCl (left) and MgO (right) due to a uniaxial stretch determined based upon ab initio calculations (solid lines) and continuum mechanics (dashed lines) as a function of pressure in the range from −3 to 30 GPa. Plotted are the three differences $\delta\Xi_{3333} - \delta\Xi_{1111}$, $\delta\Xi_{1212} - \delta\Xi_{2323}$, and $\delta\Xi_{1122} - \delta\Xi_{1133}$, which are expected to depend only on the induced deviatoric stress, τ^0.

$$\delta\Xi_{1133} = \delta\Xi_{2233} = \Xi'_{1122}(p^0 + \frac{1}{2}\tau^0), \tag{49}$$

$$\delta\Xi_{3333} = \Xi'_{1111}(p^0 + 2\tau^0), \tag{50}$$

$$\delta\Xi_{2323} = \delta\Xi_{1313} = \Xi'_{2323}(p^0 + \frac{1}{2}\tau^0), \tag{51}$$

$$\delta\Xi_{1212} = \Xi'_{2323}(p^0 - \tau^0). \tag{52}$$

In Figure 4 we compare these predictions against the ab initio calculations for a uniaxial stretch, and we conclude that the two methods are in good agreement for both NaCl and MgO within one standard deviation.

To highlight contributions of the induced deviatoric stress, we consider the following three differences:

$$\delta\Xi_{3333} - \delta\Xi_{1111} = 3\Xi'_{1111}\tau^0, \tag{53}$$

$$\delta\Xi_{1212} - \delta\Xi_{2323} = -\frac{3}{2}\Xi'_{2323}\tau^0, \tag{54}$$

$$\delta\Xi_{1122} - \delta\Xi_{1133} = -\frac{3}{2}\Xi'_{1122}\tau^0. \tag{55}$$

Note that these three differences depend only on τ^0. In Figure 5 we compare these predictions against the ab initio calculations, and we conclude that the two methods are in good agreement.

To highlight contributions of the induced pressure, we consider the following three combinations of changes in the elastic tensor:

$$\delta\Xi_{3333} + 2\delta\Xi_{1111} = 3\Xi'_{1111}p^0, \tag{56}$$

$$\delta\Xi_{1212} + 2\delta\Xi_{2323} = 3\Xi'_{2323}p^0, \tag{57}$$

$$\delta\Xi_{1122} + 2\delta\Xi_{1133} = 3\Xi'_{1122}p^0. \tag{58}$$

Note that these three combinations depend only on p^0. In Figure 6 we compare these predictions against the ab initio calculations, and we conclude that the two methods are in good agreement.

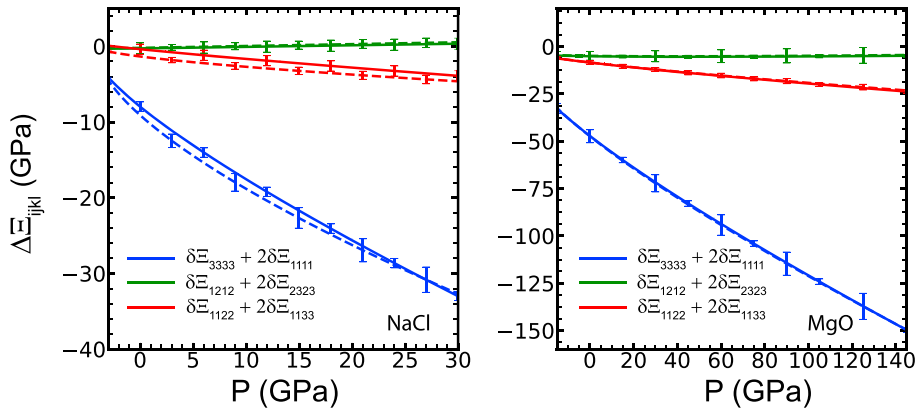

Figure 6. Comparison of combinations of changes in the elastic moduli of NaCl (left) and MgO (right) due to a uniaxial stretch determined based upon ab initio calculations (solid lines) and continuum mechanics (dashed lines) as a function of pressure in the range from −3 to 30 GPa. Plotted are the three combinations $\delta\Xi_{3333} + 2\,\delta\Xi_{1111}$, $\delta\Xi_{1212} + 2\,\delta\Xi_{2323}$, and $\delta\Xi_{1122} + 2\,\delta\Xi_{1133}$, which are expected to depend only on the induced pressure, p^0.

5. Implications for Seismic Wave Speeds

The speeds of seismic waves are determined based on a plane wave analysis of the equation of motion (9). As demonstrated by Tromp and Trampert (2018), the wave speeds are determined by the eigenvalue problem

$$\mathbf{B}\cdot\mathbf{a} = c^2\,\mathbf{a}, \tag{59}$$

where $\mathbf{B}$ denotes the symmetric Christoffel tensor with elements

$$\begin{aligned}\rho B_{j\ell} = \;& (\Gamma_{ijk\ell} + \Gamma'_{ijk\ell}\,p^0)\hat{k}_i\hat{k}_k + \frac{1}{2}\,\tau^0_{ik}\,\hat{k}_i\hat{k}_k\,\delta_{j\ell} - \frac{1}{2}\,\tau^0_{j\ell} \\ & - \frac{1}{2}\,(\Gamma'_{imk\ell}\,\tau^0_{mj} + \Gamma'_{jmk\ell}\,\tau^0_{mi})\hat{k}_i\hat{k}_k.\end{aligned} \tag{60}$$

Here $\hat{k}_i$ denotes a component of the unit plane wave vector. Because $\mathbf{B}$ is a symmetric positive-definite tensor, the eigenvalue problem (59) has three positive eigenvalues, c^2, and associated orthogonal eigenvectors, $\mathbf{a}$.

For isotropic materials, Tromp and Trampert (2018) demonstrated that the wave speeds take on the simple approximate forms

$$\rho c^2_{\mathrm{P}} = (\kappa + \kappa' p^0) + \frac{4}{3}\,(\mu + \mu' p^0) - (\kappa' + \frac{4}{3}\,\mu')\hat{\mathbf{k}}^0\cdot\boldsymbol{\tau}^0\cdot\hat{\mathbf{k}}^0, \tag{61}$$

and

$$\rho c^2_{\mathrm{S}_{1,2}} = (\mu + \mu' p^0) + \frac{1}{2}\,(1 - \mu')\hat{\mathbf{k}}^0\cdot\boldsymbol{\tau}^0\cdot\hat{\mathbf{k}}^0 - \frac{1}{2}\,(1 + \mu')\hat{\mathbf{a}}^0_{1,2}\cdot\boldsymbol{\tau}^0\cdot\hat{\mathbf{a}}^0_{1,2}. \tag{62}$$

Here $\hat{\mathbf{k}}^0$ denotes the unit wave vector prior to inducing stress, and $\hat{\mathbf{a}}^0_{1,2}$ the unit shear wave polarization directions prior to inducing stress. Note that $\hat{\mathbf{k}}^0\cdot\hat{\mathbf{a}}^0_{1,2} = 0$. Given the elastic moduli, κ and μ, and their pressure derivatives, κ' and μ', equations (61) and (62) may be used to assess the effects of induced stress on seismic wave speeds in exploration geophysics.

In global seismology, the effects of a nonhydrostatic prestress on seismic wave speeds may be accommodated as follows. Given seismologically determined profiles of compressional and shear wave speeds as a function of depth, the pressure dependence and related pressure derivatives of the elastic moduli may be determined. Thus, given $\kappa = \kappa(P)$ and $\mu = \mu(P)$ and $\kappa' = \mathrm{d}\kappa/\mathrm{d}P$ and $\mu' = \mathrm{d}\mu/\mathrm{d}P$, the effect of a deviatoric induced stress τ^0— in this case taking the form of a nonhydrostatic prestress—on seismic wave speeds is determined by

$$\rho c^2_{\mathrm{P}} = \kappa + \frac{4}{3}\,\mu - (\kappa' + \frac{4}{3}\,\mu')\hat{\mathbf{k}}^0\cdot\boldsymbol{\tau}^0\cdot\hat{\mathbf{k}}^0, \tag{63}$$

$$\rho c_{S_{1,2}}^2 = \mu + \frac{1}{2}(1-\mu')\hat{\mathbf{k}}^0 \cdot \boldsymbol{\tau}^0 \cdot \hat{\mathbf{k}}^0 - \frac{1}{2}(1+\mu')\hat{\mathbf{a}}_{1,2}^0 \cdot \boldsymbol{\tau}^0 \cdot \hat{\mathbf{a}}_{1,2}^0. \tag{64}$$

These expressions may be used to infer nonhydrostatic prestress from global seismic observations. Transverse isotropy—or a more general anisotropic background model—may be accommodated based on minor modifications, using Voigt averages for the pressure derivatives. As discussed by Tromp and Trampert (2018), the current theory used by global seismologists effectively assumes that the pressure derivatives κ' and μ' are equal to 0, rendering the compressional wave speed (63) independent of the induced deviatoric stress. The ab initio tests conducted in this study demonstrate that this is an incorrect assumption.

6. Conclusions

Motivated by a formulation commonly used in global seismology (Dahlen, 1972a, 1972b; Dahlen & Tromp, 1998), Tromp and Trampert (2018) investigated the effects of induced stress on the elastic wave equation and constitutive relation. Without employing higher-order elasticity theory (e.g., Egle & Bray, 1976; Hughes & Kelly, 1953; Murnaghan, 1951; Prioul et al., 2004) nor theories for preexisting or induced cracks (e.g., Bruner, 1976; Henyey & Pomphrey, 1982; Nur, 1971; O'Connell & Budiansky, 1974; Zheng, 2000), their formulation leads to trends observed in measurements based on laboratory data.

Here, we compare predictions of changes in the elastic moduli due to an induced stress based upon the continuum mechanics theory of Tromp and Trampert (2018) with corresponding ab initio calculations. Using NaCl and MgO—which exhibit cubic symmetry—as examples, we have shown that the continuum mechanics theory accurately predicts the effects of both induced pressure and induced deviatoric stress on elastic moduli over a wide range of background pressures.

The current theory used by global seismologists for capturing the effects of a nonhydrostatic prestress on seismic wave propagation contains two quantities, a and b, which may be chosen to obtain a particular equation of state (see Dahlen & Tromp, 1998, equations 3.135–3.137). Global seismologists prefer to choose $a = -b = 1/2$, thereby rendering the formulation independent of the hydrostatic prestress. By rewriting a and b in terms of two new parameters, namely, κ' and μ', Tromp and Trampert (2018) showed that the predicted seismic wave speeds, defined by equations (61) and (62), take on experimentally expected forms when one interprets the parameters κ' and μ' as the adiabatic pressure derivatives of the bulk and shear moduli with respect to pressure. This implies that one no longer chooses the values of a and b, but rather, these values are determined by the pressure derivatives of the moduli. The ab initio calculations presented in this paper confirm that this is the correct approach, because without such derivatives the theory fails to make accurate predictions.

Appendix A: Error Analysis

Variances for the predicted changes in the elements of the elastic tensor, $\sigma^2_{\delta\Xi_{ijk\ell}}$, based on the continuum mechanics theory are given by (Bevington & Robinson, 2003)

$$\sigma^2_{\delta\Xi_{ijk\ell}} = \sigma^2_{\Xi'_{ijk\ell}} \left(\frac{\partial \delta\Xi_{ijk\ell}}{\partial \Xi'_{ijk\ell}} \right)^2 + \sigma^2_{p^0} \left(\frac{\partial \delta\Xi_{ijk\ell}}{\partial p^0} \right)^2 + \sigma^2_{\tau^0} \left(\frac{\partial \delta\Xi_{ijk\ell}}{\partial \tau^0} \right)^2, \tag{A1}$$

where $\sigma^2_{\Xi'_{ijk\ell}}$, $\sigma^2_{p^0}$, and $\sigma^2_{\tau^0}$ are the variances for $\Xi'_{ijk\ell}$, p^0, and τ^0, respectively. Changes in the elastic tensor, $\delta\Xi_{ijk\ell}$, are given by (40)–(42) for an induced pressure and by (47)–(51) for an induced uniaxial stretch. The variances $\sigma^2_{p^0}$ and $\sigma^2_{\tau^0}$ are obtained by propagating the errors for expressions (44) and (45):

$$\sigma^2_{p^0} = \frac{1}{9}(\epsilon^0)^2 \left(\sigma^2_{\Xi_{1111}} + 4\sigma^2_{\Xi_{1122}} \right), \tag{A2}$$

and

$$\sigma^2_{\tau^0} = \frac{1}{9}(\epsilon^0)^2 \left(\sigma^2_{\Xi_{1111}} + \sigma^2_{\Xi_{1122}} \right). \tag{A3}$$

The variances $\sigma^2_{\Xi_{1111}}$ and $\sigma^2_{\Xi_{1122}}$ are determined by fitting the mean squared error of the corresponding elastic coefficient to equation (34):

$$\sigma^2_{\Xi_{ijk\ell}} = \frac{1}{N}\sum\left(\Xi^{\text{fit}}_{ijk\ell} - \Xi^{\text{ab initio}}_{ijk\ell}\right)^2, \tag{A4}$$

Here $\Xi^{\text{fit}}_{ijk\ell}$ and $\Xi^{\text{ab initio}}_{ijk\ell}$ are the elastic coefficients obtained based on equation (34) and the ab initio calculations, respectively, and N denotes the number of pressures calculated computationally. Variances for the pressure derivatives are determined by

$$\frac{\sigma'^2_{\Xi_{ijk\ell}}}{\Xi'^2_{ijk\ell}} = \frac{\sigma^2_g}{g^2} + \frac{\sigma^2_\kappa}{\kappa^2}, \tag{A5}$$

where σ^2_κ is the variance for κ and g the numerator of equation (35). Thus,

$$\sigma^2_g = \sigma^2_{\Xi^0}\left(\frac{\partial g}{\partial \Xi^0}\right)^2 + \sigma^2_f\left(\frac{\partial g}{\partial f}\right)^2 + \sigma^2_{\Xi'^0}\left(\frac{\partial g}{\partial \Xi'^0}\right)^2. \tag{A6}$$

Here $\sigma^2_{\Xi^0}$ and $\sigma^2_{\Xi'^0}$ are the variances for the fitting parameters of equation (34), and σ^2_f is given by

$$\sigma^2_f = \frac{1}{9}\left(\frac{\sigma_{V^0}}{V^0}\right)^2\left(\frac{V^0}{V}\right)^{\frac{4}{3}}. \tag{A7}$$

Here $\sigma^2_{V^0}$ is the variance for V^0, obtained via fitting equation (29) to the calculated data. Thus, we have the necessary ingredients to calculate the errors in the predicted $\delta\Xi_{ijk\ell}$ based on equation (A1).

Errors for the ab initio calculations are determined using the fitted mean squared error of each elastic coefficient. Errors in pressure are obtained based on the difference between equation (31) and the trace of the stress tensor. Thus, variances for $\delta\Xi_{ijk\ell}$ obtained via the ab initio calculations are determined by

$$\sigma^2_{\delta\Xi^{\text{ab initio}}_{ijk\ell}} = \sigma^2_{\Xi^u_{ijk\ell}} + \sigma^2_{\Xi^s_{ijk\ell}} + \sigma^2_P, \tag{A8}$$

where $\sigma^2_{\Xi^u_{ijk\ell}}$ and $\sigma^2_{\Xi^s_{ijk\ell}}$ are the variances given by equation (A4) for the unstrained and strained configurations, respectively, and σ^2_P is the variance in pressure.

Acknowledgments
We thank Tom Duffy and Yanadet Sripanich for fruitful discussions and advice. Comments and suggestions by Yves Guéguen and an anonymous reviewer helped to improve the manuscript. The research leading to these results has received funding from the European Research Council (ERC) under the European Union's Seventh Framework Programme (FP/2007-2013) grant agreement 320639 (iGEO). R. M. W. and M. L. M. were supported by NSF grants EAR-1503084 and EAR-1348066. The data used in this article may be accessed via the Coalition on Publishing Data in the Earth and Space Sciences https://copdessdirectory.osf.io/.

References

Barron, T. H. K., & Klein, M. L. (1965). Second-order elastic constants of a solid under stress. *Proceedings of the Physical Society*, *85*, 523–532.
Bevington, P. R., & Robinson, D. K. (2003). *Data reduction and error analysis for the physical sciences* (3rd ed.). New York, U.S.A.: McGraw-Hill Higher Education.
Birch, F. (1961). The velocity of compressional waves in rocks to 10 kilobars: 2. *Journal of Geophysical Research*, *66*, 2199–2224.
Bogardus, E. H. (1965). Third-order elastic constants of Ge, MgO, and fused SiO2. *Journal of Applied Physics*, *36*, 2504–2513. Retrieved from https://aip.scitation .org/doi/abs/10.1063/1.1714520 https://doi.org/10.1063/1.1714520
Bruner, W. M. (1976). Comment on "Seismic velocities in dry and saturated cracked solids" by Richard J. O'Connell and Bernard Budiansky. *Journal of Geophysical Research*, *81*, 2573–2576.
Dahlen, F. A. (1972a). Elastic dislocation theory for a self-gravitating elastic configuration with an initial static stress field. *Geophysical Journal International*, *28*, 357–383.
Dahlen, F. A. (1972b). Elastic velocity anisotropy in the presence of an anisotropic initial stress. *Bulletin of the Seismological Society of America*, *62*, 1183–1193.
Dahlen, F. A., & Tromp, J. (1998). *Theoretical global seismology*. New Jersey: Princeton U. Press.
Eberhart-Phillips, D., Han, D.-H., & Zoback, M. D. (1989). Empirical relationships among seismic velocity, effective pressure, porosity, and clay content in sandstone. *Geophysics*, *54*, 82–89.
Egle, D. M., & Bray, D. E. (1976). Measurement of acoustoelastic and third-order elastic constants for rail steel. *Journal of the Acoustical Society of America*, *60*, 741–744.
Fazio, T. D., Aki, L., & Alba, K. (1973). Solid earth tide and observed change in the in situ seismic velocity. *Journal of Geophysical Research*, *78*, 1319–1322.
Giannozzi, P., Baroni, S., Bonini, N., Calandra, M., Car, R., Cavazzoni, C., et al. (2009). Quantum espresso: A modular and open-source software project for quantum simulations of materials. *Journal of Physics: Condensed Matter*, *21*(39), 395502.
Henyey, F. S., & Pomphrey, N. (1982). Self-consistent elastic moduli of a cracked solid. *Geophysical Research Letters*, *81*, 903–906.
Hohenberg, P., & Kohn, W. (1964). Inhomogeneous electron gas. *Physical Review*, *136*(3B), B864–B871. https://doi.org/10.1103/PhysRev.136.B864
Hughes, D. S., & Kelly, J. L. (1953). Second-order elastic deformation of solids. *Physical Review*, *92*, 1145–1149.
Johnson, P. A., & Rasolofosaon, P. N. J. (1996). Nonlinear elasticity and stress-induced anisotropy in rock. *Geophysical Research Letters*, *101*, 3113–3124.
Karki, B. B., Stixrude, L., & Wentzcovitch, R. M. (2001). High-pressure elastic properties of major materials of Earth's mantle from first principles. *Reviews of Geophysics*, *39*(4), 507–534. https://doi.org/10.1029/2000RG000088

Kohn, W., & Sham, L. J. (1965). Self-consistent equations including exchange and correlation effects. *Physical Review*, *140*(4A), A1133–A1138. https://doi.org/10.1103/PhysRev.140.A1133

Murnaghan, F. D. (1951). *Finite deformation of an elastic solid*. Mineola, New York: Dover Publications Inc.

Nielsen, O. H., & Martin, R. M. (1985). Quantum-mechanical theory of stress and force. *Physical Review B*, *32*(6), 3780–3791. https://doi.org/10.1103/PhysRevB.32.3780

Nur, A. (1971). Effects of stress on velocity anisotropy in rocks with cracks. *Geophysical Research Letters*, *76*, 2022–2024.

Nur, A., & Simmons, G. (1969). Stress-induced velocity anisotropy in rock: An experimental study. *Geophysical Research Letters*, *74*, 6667–6674.

O'Connell, R. J., & Budiansky, B. (1974). Seismic velocities in dry and saturated cracked solids. *Geophysical Research Letters*, *79*, 5412–5426.

Poirer, J. P. (2000). *Introduction to the physics of the Earth's interior* (2nd ed.). Cambridge, U.K.: Cambridge University Press.

Prioul, R., Bakulin, A., & Bakulin, V. (2004). Nonlinear rock physics model for estimation of 3D subsurface stress in anisotropic formations: Theory and laboratory verification. *Geophysics*, *69*, P.415–425.

Renaud, G., Le Bas, P. Y., & Johnson, P. A. (2012). Revealing highly complex elastic nonlinear (anelastic) behaviour of Earth materials applying a new probe: Dynamic acoustoelastic testing. *Journal of Geophysical Research*, *117*, B06202. https://doi.org/10.1029/2011JB009127

Silver, P. G., Daley, T. M., Niu, F., & Majer, E. L. (2007). Active source monitoring of cross-well seismic travel time for stress-induced changes. *Bulletin of the Seismological Society of America*, *97*, 281–293.

Telichko, A. V., Erohin, S. V., Kvashnin, G. M., Sorokin, P. B., Sorokin, B. P, & Blank, V. D. (2017). Diamond's third-order elastic constants: Ab initio calculations and experimental investigation. *Journal of Materials Science*, *53*, 3447–3456. Retrieved from https://link.springer.com/article/10.1007/s10853-016-0633-x\#citeas https://doi.org/10.1007/s10853-016-0633-x

Tromp, J., & Trampert, J. (2018). Effects of induced stress on seismic forward modelling and inversion. *Geophysical Journal International*, *213*, 851–867.

Verdon, J. P., Angus, D. A., Kendall, M. J., & Hall, S. A. (2008). The effect of microstructure and nonlinear stress on anisotropic seismic velocities. *Geophysics*, *78*, D41–D51.

Wang, H., & Li, M. (2009). Ab initio calculations of second-, third-, and fourth-order elastic constants for single crystals. *Physical Review B*, *79*, 224102. Retrieved from https://journals.aps.org/prb/pdf/10.1103/PhysRevB.79.224102 https://doi.org/10.1103/PhysRevB.79.224102

Wentzcovitch, R. M. (1991). Invariant molecular-dynamics approach to structural phase transitions. *Physical Review B*, *44*, 69–61. Retrieved from https://link.aps.org/doi/10.1103/PhysRevB.44.2358 https://doi.org/10.1103/PhysRevB.44.2358

Wentzcovitch, R. M., Martins, J. L., & Price, G. D. (1993). Ab initio molecular-dynamics with variable cell-shape—Application to $MgSiO_3$. *Physical Review Letters*, *70*, 3947–3950. Retrieved from https://link.aps.org/doi/10.1103/PhysRevLett.70.3947 https://doi.org/10.1103/PhysRevLett.70.3947

Wentzcovitch, R. M., & Price, G. D. (1996). High pressure studies of Mantle minerals by ab initio variable cell shape molecular dynamics. *Molecular Engineering*, *6*, 69–61. Retrieved from https://doi.org/10.1007/BF00161722 https://doi.org/10.1007/BF00161722

Wentzcovitch, R. M., Wu, Z., & Carrier, P (2010). First principles quasiharmonic thermoelasticity of mantle minerals. *Reviews in Mineralogy and Geochemistry*, *71*, 99–128.

Zheng, Z. (2000). Seismic anisotropy due to stress induced cracks. *International Journal of Rock Mechanics and Mining Sciences*, *37*, 39–49.